Appendix B. Details on the null communities.

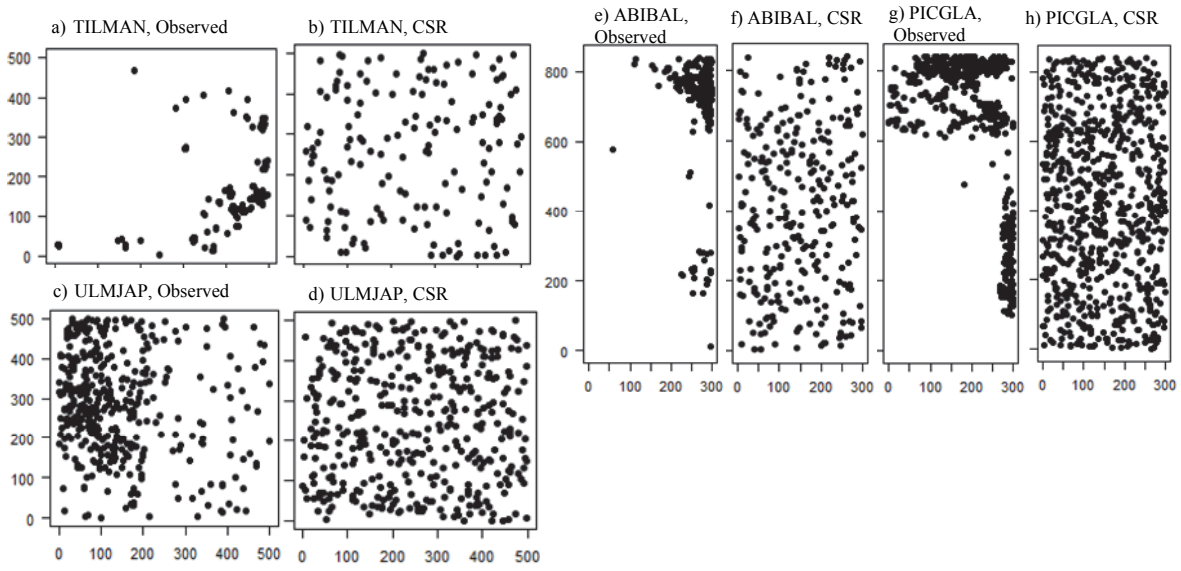

FIG. B1. Examples for observed species distribution patterns (Panels a, c, e, and h) and the corresponding null distribution patterns (Panels b, d, f, and h) of the random placement hypothesis (CSR). Panels a-d show examples for the CBS plot and panels e–h of the Wabikon forest.

Homogeneous Poisson process for random placement *hypothesis*

This hypothesis assumes that the null community would be assembled in absence of spatially structuring processes (i.e., no habitat filtering, absence of species interactions, and no clustering mechanisms) and represents therefore a point of reference for the evaluation of more complex null communities. To represent the random placement hypothesis we displaced the individuals of each species to random locations within the observation window *W* (Fig. B1). This null model is called in spatial statistics homogeneous Poisson process (Illian et al. 2008).

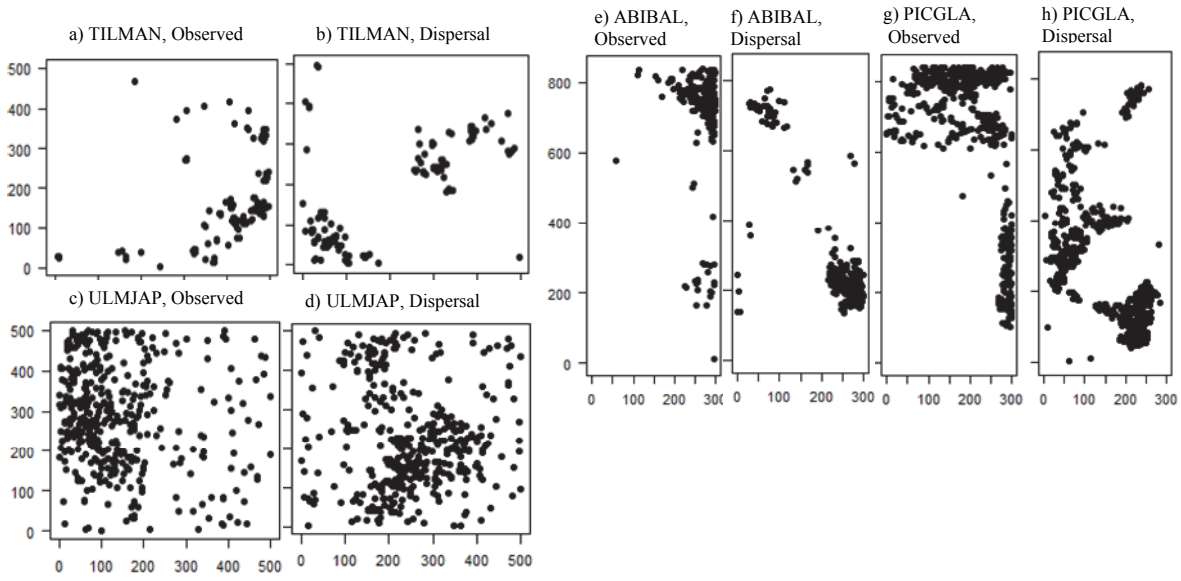

FIG. B2. Examples for observed species distribution patterns (Panels a, c, e, and h) and the corresponding null distribution patterns (Panels b, d, f, and h) of the dispersal limitation hypothesis. Panels a-d show examples for the CBS plot and panels e-h of the Wabikon forest.

Pattern reconstruction for dispersal limitation hypothesis

This hypothesis assumes that the null community would be assembled only by action of dispersal limitation and other internal mechanisms of population dynamics that cause species clustering, but not by habitat filtering or species interactions. To represent this hypothesis we need a null model that generates null distribution patterns that show exactly the same cluster properties as the observed pattern, but represent stochastic replicates of the observed pattern. Previous studies accomplished this by fitting the parametric Thomas cluster processes to the observed pattern and using realizations of the fitted process as null patterns (Shen et al. 2009; Wang et al. 2011, 2013). However, the Thomas process yields in general only a rough approximation of the observed

clustering of the species and may miss out important properties of the pattern (e.g., Wiegand et al. 2013).

In this study we use non-parametric techniques of pattern reconstruction (Rintoul and Torquato 1997; Tscheschel and Stoyan 2006; Illian et al. 2008; Wiegand et al. 2013) as solution to the problem of generating species patterns that show the same stochastic characteristics as the observed pattern. To this end we used the pattern reconstruction algorithm described in Wiegand et al. (2013) that is based on methods presented in Tscheschel and Stoyan (2006). This algorithm is a variation of simulated annealing (Kirkpatrick et al. 1983) that generates by trial and error a series of patterns that approach in each simulation step the summary statistics of the observed patterns more closely. The statistical properties of the observed pattern φ are measured by several functional summary statistics $f_i^{\varphi}(x)$ where the variable x may represent distance r. During each simulation step t we estimated the corresponding summary statistics $f_i^{\psi_t}(x)$ of the simulated pattern ψ_t to estimate the deviations

$$E_i^{\varphi}(\psi_t) = \sqrt{\frac{1}{n_i}\sum_{b=1}^{n_i}[f_i^{\varphi}(x_b) - f_i^{\psi_t}(x_b)]^2} \qquad \text{(B.1)}$$

between $f_i^{\varphi}(x)$ and $f_i^{\psi_t}(x)$ where the variable x is evaluated at n_i discrete values x_b. To combine the deviations $E^{\varphi}{}_i$ arising from different summary statistics i into a total deviation measure we need to normalize with weights w_i in a way that the different summary statistics yielded approximately the same value of $E^{\varphi}{}_i$ if the observed and simulated patterns approached a good agreement (for details see Wiegand et al. 2013). The total deviation yields:

$$E^{\varphi}_{total}(\psi_t) = \frac{\sum_{i=1}^{I} w_i E^{\varphi}_i(\psi_t)}{\sum_{i=1}^{I} w_i} \qquad \text{(B.2)}$$

The reconstruction of pattern φ starts with a random pattern ψ_0 that has the same number of points as φ. In each simulation step t a randomly selected point is tentatively removed and a new point with random coordinates is proposed instead. This new point is accepted if $E^{\varphi}_{total}(\psi_t) < E^{\varphi}_{total}(\psi_{t-1})$, otherwise another new point is considered (Tscheschel and Stoyan 2006; Wiegand et al. 2013). Thus, the new pattern ψ_t is slightly more similar to the observed pattern than the previous pattern ψ_{t-1}. This algorithm is able to find local minima with very small total deviation (Wiegand et al. 2013) and each simulation will end up in a different local minimum (the absolute minimum would be the observed pattern φ).

The pattern reconstruction algorithm therefore generates the stochastic replicates of the observed pattern required for the independence null model. The resulting patterns very closely resemble the possibly complex spatial structure of the observed species distribution pattern, but do not account for potential habitat associations (Fig. B2).

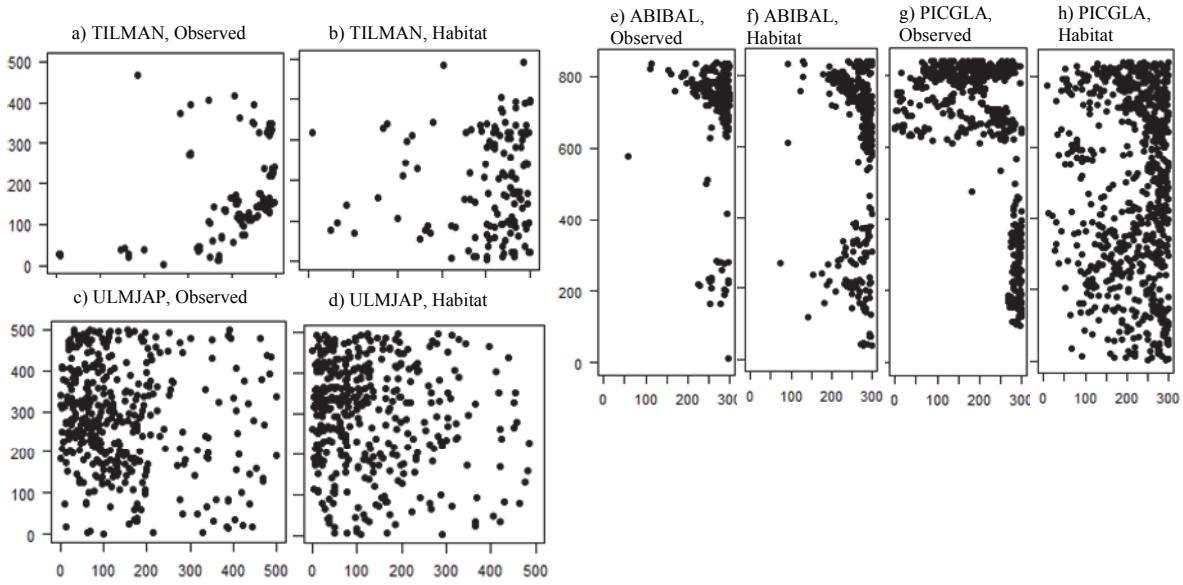

FIG. B3. Examples for observed species distribution patterns (Panels a, c, e and h) and the corresponding null distribution patterns (Panels b, d, f, and h) of the habitat filtering hypothesis. Panels a-d show examples for the CBS plot and panels e–h of the Wabikon forest.

Heterogeneous Poisson process for habitat filtering hypothesis

This hypothesis assumes that the species distributions of the null community follow exclusively their habitat suitability, as determined by the joined action of different environmental variables. We used log-linear regression models to estimate the intensity function $\lambda_i(\mathbf{x})$ that represents habitat suitability of species *i* based on environmental covariates (topography, neighboring tree species, and soils).

To estimate the intensity function $\lambda_i(\mathbf{x})$ we used three topographic factors (elevation, slope and aspect) and tree density per quadrat (5m×5m) for the Wabikon plot, and included the first two principal components (PCs) from the eight soil factors for the CBS plot as environmental factors. The first two PCs explained 86.6% of total variance in soil factors, which

can reduce possible overfitting. The intensity function was then fitted for each species using maximum likelihood estimation in the following form (Waagepetersen and Guan 2009):

$$\lambda(\mathbf{x}) = \exp(\beta_0 + \beta_1 v_1(\mathbf{x}) + \ldots + \beta_n v_n(\mathbf{x})) \qquad \text{(B.3)}$$

with coefficiensts β_j and the environmental factor $v_j(\mathbf{x})$, where n = 4 for the Wabikon plot, and n = 6 for the CBS plot. We generated null distribution patterns by randomly relocating the individuals of all species within W, but accepting a given location only with probability $\lambda_i(\mathbf{x})/\lambda_i^*$ where λ_i^* is the maximal value of $\lambda_i(\mathbf{x})$ in W. The resulting null distribution patterns reflect the underlying habitat association but do not show additional clustering (Fig. B3). This null model is called heterogeneous Poisson process (Illian et al. 2008).

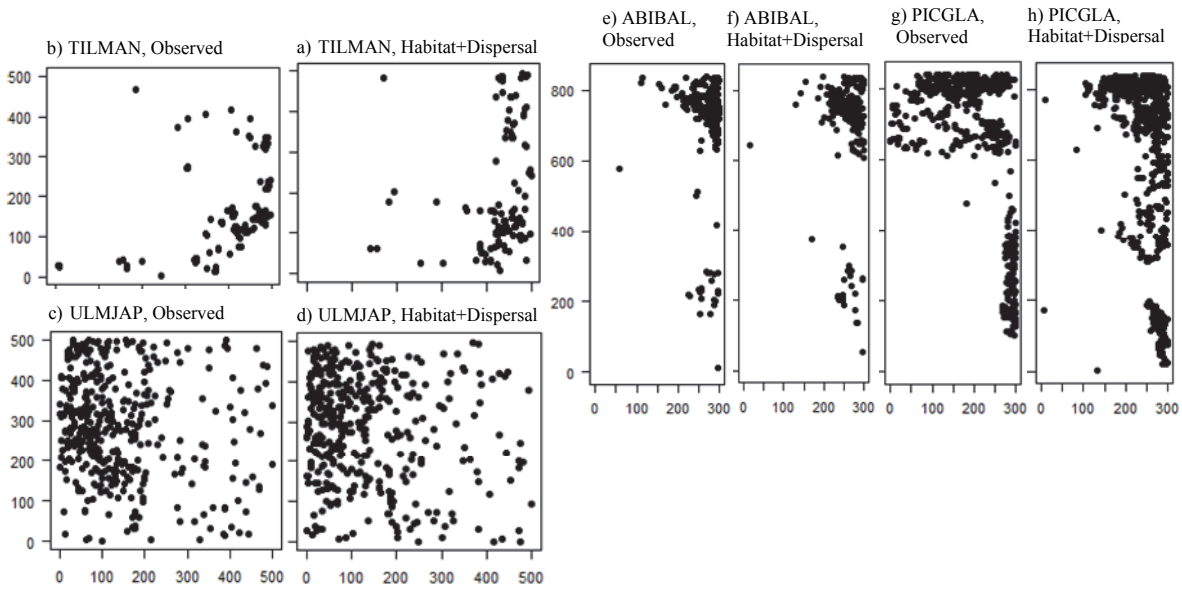

FIG. B4. Examples for observed species distribution patterns (Panels a, c, e and h) and the corresponding null distribution patterns (Panels b, d, f, and h) of the combined habitat filtering and dispersal limitation hypothesis. Panels a–d show examples for the CBS plot and panels e–h of the Wabikon forest.

Pattern reconstruction for combined habitat filtering and dispersal limitation hypothesis

This hypothesis assumes that the community is assembled by the joined action of internal cluster mechanisms and habitat filtering. We generated the corresponding null distribution patterns similar to that of the dispersal limitation hypothesis, but constrained the pattern reconstruction algorithm additionally with the intensity function $\lambda_i(\mathbf{x})$ derived in the habitat filtering hypothesis (Wiegand et al. 2013). Basically, the annealing algorithm described above is used to minimize the differences in several summary statistics between the observed and the reconstructed pattern (in our case up to distances of 200m and 120m for the CSB and Wabikon forest, respectively). However, the extended algorithm that considers the intensity function $\lambda_i(\mathbf{x})$ starts with a pattern generated by a heterogeneous Poisson process (i.e., the habitat filtering hypothesis) that has the same number of points as the original pattern. In each simulation step of the annealing algorithm, a randomly selected point is tentatively removed and a new point following the above rules of the heterogeneous Poisson process is proposed instead. This new point is accepted, as described above in "*Pattern reconstruction for dispersal limitation hypothesis*", if the mean deviance between the observed and the simulated summary characteristics decreased (Tscheschel and Stoyan 2006; Illian et al. 2008), otherwise it is removed and another new point is selected. The null distribution patterns therefore faithfully reflect the observed signal of association of the species to our environmental variables and its observed clustering (Fig. B4). Departures from this hypothesis may be caused by unobserved environmental variables that are missed in the habitat model and by species interactions.

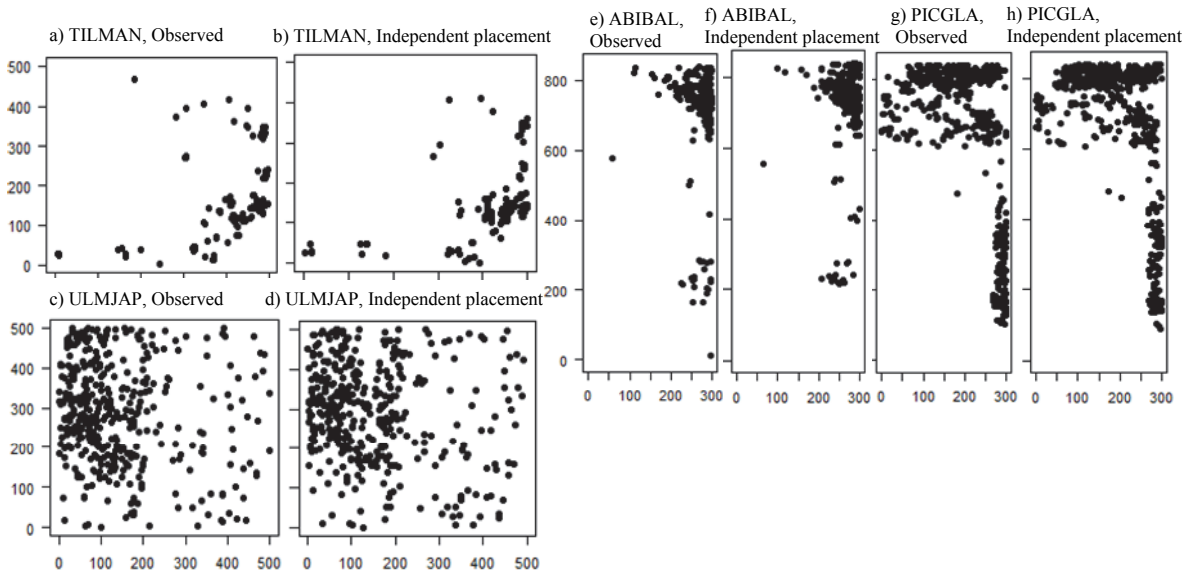

FIG. B5. Examples for observed species distribution patterns (Panels a, c, e, and h) and the corresponding null distribution patterns (Panels b, d, f, and h) of the independent placement hypothesis. Panels a–d show examples for the CBS plot and panels e–h of the Wabikon forest.

Pattern reconstruction for independent placement hypothesis

To study the "pure" effects of interspecific interactions, the null model must be conditioned on the observed variation in the intensity function $\lambda(\boldsymbol{x})$ of the focal species but not on a parametrically estimated intensity function as for the combined habitat filtering and dispersal limitation hypothesis. This can be done by using a non-parametric kernel estimate of $\lambda(\boldsymbol{x})$ with bandwidth R (Wiegand et al. 2013) instead of the parametric estimation of $\lambda(\boldsymbol{x})$. This approach counts basically all individuals within distance R of a target location $\boldsymbol{x}$ and divides by the area πR^2 to obtain $\lambda(\boldsymbol{x})$. This procedure averages over potential small-scale variation in tree placement caused by species interactions, but maintains larger-scale variation in the intensity function as caused for example by habitat association and dispersal limitation. This allows us to detect

signatures of small-scale species interactions at distances r shorter than the bandwidth R. Pattern reconstruction that additionally conditions on the observed intensity function (Wiegand et al. 2013) can thus be used as null model of independence. We used a bandwidth of R = 50m which is somewhat larger than the typical range of species interactions in forests (Wang et al. 2010). Thus, the null communities will show only for distances below 50m departures from the observed beta diversity.

The resulting null model patterns show the same larger scale distribution pattern as that observed for the focal species (i.e., the same areas of the plot have low or high densities of the focal species), and the typical small-scale structures re-appear, but at somewhat displaced locations (Fig. B5). The procedure to obtain null distribution patterns based on pattern reconstruction is the same as described above for the combined habitat filtering and dispersal limitation hypothesis; the only difference is that the intensity function is based on a non-parametric estimator.

LITERATURE CITED

Illian, J., A. Penttinen, H. Stoyan, and D. Stoyan. 2008. Statistical Analysis and Modeling of Spatial Point Patterns. Chichester:Wiley.

Rintoul, M. D., and S. Torquato. 1997. Reconstruction of the structure of dispersions. Journal of Colloid and Interface Science 186:467–476.

Shen, G., M. Yu, X. Hu, X. Mi, H. Ren, I. Sun, and K. Ma. 2009. Species-area relationships explained by the joint effects of dispersal limitation and habitat heterogeneity. Ecology 90:3033–3041.

Tscheschel, A., and D. Stoyan. 2006. Statistical reconstruction of random point patterns. Computional Statistics & Data Analysis 51:859–871.

Waagepetersen, R., and Y. Guan. 2009. Two-step estimation for inhomogeneous spatial point processes. Journal of the Royal Statistical Society, Series B 71:685–702.

Wang, X., N. G. Swenson, T. Wiegand, A. Wolf, R. Howe, F. Lin, J. Ye, Z. Yuan, S. Shi, X. Bai, D. Xing, and Z. Hao, 2013. Phylogenetic and functional diversity area relationships in two temperate forests. Ecography 36:883–893.

Wang, X., T. Wiegand, A. Wolf, R. Howe, S. J. Davies, and Z. Hao. 2011. Spatial patterns of tree species richness in two temperate forests. Journal of Ecology 99:1382–1393.

Wang, X., T. Wiegand, Z. Hao, B. Li, J. Ye, and F. Lin. 2010. Species associations in an old-growth temperate forest in north-eastern China. Journal of Ecology 98:674–686.

Wiegand, T, F. He, and S. P. Hubbell. 2013. A systematic comparison of summary characteristics for quantifying point patterns in ecology. Ecography 36:92–103.